

Improved Apparatus for Dynamic Column Breakthrough Measurements Relevant to Direct Air Capture of CO₂

W. Sean McGivern,* Huong Giang T. Nguyen, and Jeffrey A. Manion*

*Chemical Sciences Division, National Institute of Standards and Technology, Gaithersburg,
MD*

E-mail: sean.mcgivern@nist.gov; jeffrey.manion@nist.gov

Abstract

Dynamic column breakthrough (DCB) measurements are valuable for characterizing the adsorption of gaseous species by solid sorbents and are typically used for high concentrations of adsorptives, often at elevated temperatures and pressures. However, adsorbents for the direct capture of carbon dioxide from natural air demand measurement capability at low partial pressures of CO₂ at atmospherically relevant temperatures and pressures. We have developed a new apparatus focused on the measurement of DCB curves under typical tropospheric conditions. The new apparatus is described in detail and validated with breakthrough curve measurements. Adsorption capacities are reported at (233.1 to 323.1) K and (351 to 1078) hPa for low carbon dioxide concentrations on 13X zeolite samples on the order of a few hundred milligrams. Measurement uncertainties related to timing, flow, temperature, and concentrations are analyzed and the present results at 273 K, 298 K, and 323 K are compared with static measurements obtained with a manometric adsorption analyzer. In addition, experiments at a typical atmospheric CO₂ concentration of 400 μL · L⁻¹ have been performed.

Introduction

The capture of carbon dioxide (CO₂) directly from free atmosphere (direct air capture, DAC) represents an important process for the overall mitigation of global warming. Recent effort in the study of carbon sequestration has focused on point-source capture from combustion plants due in part to the difficulty of DAC on a large scale.¹ However, recent analyses have demonstrated the feasibility and value of capturing CO₂ directly for permanent storage.² In particular, by offsetting emissions from difficult to eliminate sources, e.g. from agricultural waste, aviation, and long-haul shipping, DAC will play a critical role in achieving a net-zero CO₂ portfolio.³ Ultimately, successful development and scaling of DAC processes could provide a methodology to reduce atmospheric CO₂ concentrations and actively reverse anthropogenic warming. To enable such long-term mitigation strategies to succeed, it is imperative that current research focus on DAC carbon capture in addition to point-source capture.

The demands of a direct air capture (DAC) adsorbent differ from those used for adsorption from a point source. In particular, DAC must take place at the low CO₂ concentrations of free air under tropospheric conditions that span a wide range of temperatures, pressures, and relative humidities. The experimental criteria for a DAC instrument, which essentially reflect atmospheric conditions both at ground level and aloft, are provided in Table 1.

Table 1: Conditions for measurements relevant to DAC

| Figure of Merit | Range | Units |
|-------------------------------|-----------------|-----------------------------------|
| Temperature | -233.1 to 323.1 | K |
| Pressure | 300 to 1050 | hPa |
| Relative Humidity | 0 to 80 | % |
| CO ₂ Concentration | 400 | $\mu\text{L} \cdot \text{L}^{-1}$ |

Many of these conditions are not conducive to high adsorption capacity, including low CO₂ concentrations, low pressures, and the presence of large quantities of H₂O at elevated humidities. These are, however, the conditions under which DAC must take place, and the present experimental design focuses on satisfying these criteria to permit evaluation of

sorbents that can be used for DAC.

For systems involving the interaction of a gas with a solid adsorbent, a critical measurement for evaluating adsorbent materials is a dynamic column breakthrough (DCB) curve, which is a plot of the time-dependent concentration of an adsorptive in the effluent of a gas passing through a bed of adsorbent. It is thus quantitatively related to the time-dependent uptake efficiency. DCB curves are measured by initiating the exposure of a known quantity of sample adsorbent to a flow of adsorptives at fixed concentrations and monitoring the post-column concentrations until all species have reached their equilibrium inlet concentrations (i.e. the adsorbent is completely saturated). From these curves, the adsorption capacity of the sample material may be determined directly from the known inlet concentrations and molar flow rates. In addition, equilibria of multi-component systems and kinetic data may be derived from the DCB curves by mathematical modeling of the adsorption systems.^{4,5}

In this study, we present a new apparatus for measuring DCB curves with small sorbent sizes (< 500 mg) and a focus on the DAC-relevant temperature and pressure ranges in Table 1 without considering relative humidity, which will be explored in a future publication.

In designing the instrument, we have focused on two major goals that reflect ideal cases: the presentation of a step function in concentration to the head of the column and the accurate measurement of the concentration profile at the column outlet by minimizing dispersion. DCB curves measured under such conditions will be maximally informative in adsorption modeling. We have chosen to characterize the system by measuring breakthrough curves for 13X zeolite using a 1.0% mixture of CO_2 in helium (He). For these curves, we present equilibrium capacity of CO_2 on the sorbent to demonstrate the system's capability in the absence of adsorption modeling and compare these results to independent static capacity measurements. A concentration of 1.0% CO_2 was chosen for characterization rather than $400 \mu\text{L} \cdot \text{L}^{-1}$ to yield a higher adsorptive partial pressure, providing a larger variation in capacities over the temperature and total pressure ranges utilized while still remaining in a low-pressure region of the adsorption isotherm. We also present a $400 \mu\text{L} \cdot \text{L}^{-1}$ CO_2 in He

curve to demonstrate the low-concentration capability of the newly constructed apparatus.

Experiment

Materials

The main flow paths, fittings, and other wetted parts of the present apparatus are constructed with 316 stainless steel (SS) with the rotary valve bodies constructed from NITRONIC[®] 60 (Cleveland-Cliffs, Cleveland, OH) SS.⁶ Valve seats are polytetrafluoroethylene (PTFE) with the rotary valves utilizing a proprietary reinforced PTFE material (Valcon E2, Vici Valco, Houston, TX). The mass flow controllers utilize fluorocarbon rubber (Viton[®], Chemours, Wilmington, DE) for valve sealing. Unless otherwise noted, tubing is 316 SS (Swagelok, Solon, OH) of 6.35 mm outer diameter (o. d.). The inner diameter (i. d.) of the tubing varies based on the location; 3.86 mm i. d. tubing is used throughout the postcolumn region to closely match the rotary valve port size (see below) and more common thin-walled 4.57 mm i. d. is used elsewhere. Connectors are matched to this size. Depending on location and purpose, connections are made with Swagelok compression fittings, Valco zero dead volume compression fittings, or Swagelok VCR[®] gasket seal fittings that were orbitally welded into the manifold to ensure a smooth flow path. Specific commercial instruments employed in the apparatus are described later as necessary.

Apparatus

Conceptually, the methodology employed here to measure DCB curves is straightforward. One first establishes a flow of gas containing a fixed concentration of adsorptive and, at a specified time, directs that flow through one of two temperature-controlled columns, either a column containing the sorbent of interest or an otherwise identical one that is empty (the blank). The time-dependent compositions of the postcolumn gas streams are monitored and the behavior of the sorbent-containing system compared with that of the blank, leading

directly to the DCB curve of the sorbent. To flush the flow paths between experiments and to carry out *in situ* activation of the sorbent, a second inlet of an inert purge gas is added and a system of valves and tees is used to direct the two gas flows. While straightforward in principle, experimental challenges include precisely controlling the pressure and temperature conditions, obtaining high quality analytical data for all species of interest, and avoiding confounding influences on the data caused by dead volumes, pressure spikes, diffusion, flow eddies, etc. It is these latter issues that strongly affect data quality, including measurement repeatability and uncertainty.

The design of the present apparatus in part follows that presented by Wilkins et al.⁵ with several key modifications. The initial discussion below focuses on the specific instruments used in the apparatus. A discussion of differences between the present apparatus to the literature design follows. A schematic of the system is provided in Figure 1.

An input manifold is used to establish the composition of the sample gas containing an adsorptive of interest that will be directed to the columns. The manifold consists of mass flow controllers (MC-Series, Alicat, Tuscon, AZ) connected to pressure-regulated gas cylinders and a network of tubing and valves. For each component, the desired sample concentrations are matched to a controller flow rate range that will ensure accuracy: $1000 \text{ cm}^3 \cdot \text{min}^{-1}$ for He, $100 \text{ cm}^3 \cdot \text{min}^{-1}$ for N₂, and $5 \text{ cm}^3 \cdot \text{min}^{-1}$ and $0.5 \text{ cm}^3 \cdot \text{min}^{-1}$ for CO₂ (throughout this work, volumetric flow rates are reported at 273.15 K and 101.325 kPa, the standard temperature and pressure (STP) recommended by the International Union of Pure and Applied Chemistry [IUPAC]). Gases can be individually isolated via pneumatic bellows-sealed diaphragm valves (Swagelok). Precolumn pressures are measured at the input manifold outlet using a precision sensor (CPT6100, Mensor LP, San Marcos, TX), indicated as P₁ in Figure 1. Stirring induced at the mass flow controller tees and diffusion in the subsequent tubing are sufficient to effectively mix the sample gases prior to reaching the columns.

Separate from the sample gas input, the apparatus has a second inlet for directing a flow of He purge gas through the columns. This flow is controlled by a $1000 \text{ cm}^3 \cdot \text{min}^{-1}$

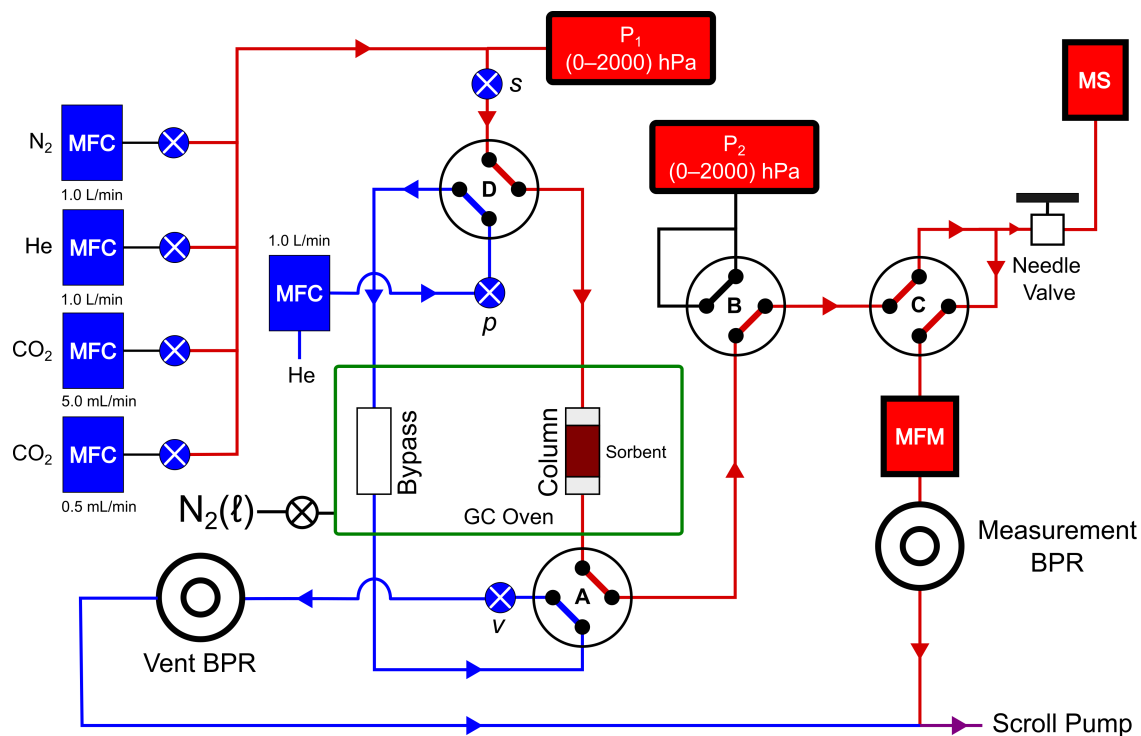


Figure 1: Schematic of NIST Dynamic Column Breakthrough Apparatus. Valve orientations and gas flow paths (red for sample and blue for purge) correspond to those at initiation of a sorbent column adsorption experiment (i.e. t_0). Bold letters identify two-way, four-port rotary valves, and crossed circles are on-off valves with some labeled for reference in the text. MFC and MFM are mass flow controllers and meters, respectively. MS is the mass spectrometer, P_1 and P_2 indicate manometers of the total system pressure, and BPR refers to the backpressure regulators.

mass flow controller. The purge helium is used to sweep the columns of sample gas between experiments, thus establishing measurement baselines, and for adsorbent activation procedures. Diaphragm valves *s* and *p* are used for on-off control of the flows of sample and purge gases into the system. Rotary valve **D** directs the inlet flow of sample and purge gas to the parallel sorbent and bypass columns. Postcolumn gas flow paths, discussed further below, are controlled by rotary valves **A**, **B**, and **C**. For temperature control, the columns are located within the oven of an Agilent 6890 gas chromatograph (GC), which can be set to temperatures ranging from -80°C to 450°C . For temperatures below ambient, the oven is cooled by a GC-controlled inflow of cold nitrogen from a liquid N_2 tank.

The sorbent and bypass columns are constructed from a pair of 6.35 mm Swagelok VCR welding glands connected through a Swagelok compression tee with a capped cross port (to be used in future temperature studies). For the sorbent column, the sorbent is placed after the tee cross port and is surrounded by lightly packed quartz wool. The bypass column is left empty. Both columns are then sealed into flow manifold via nickel gaskets containing $60\ \mu\text{m}$ frits (Swagelok). In the sorbent column, the frits ensure that sorbent material cannot pass into the flow manifold, while on the bypass column they balance the pressure drops across the two columns so that observed pressure differences are due solely to the sorbent bed and quartz wool packing. The VCR fittings permit the easy exchange of sample cells and allow columns of different length and diameter to be used if significantly different sorbent amounts are to be tested.

We have utilized a rotary 4-port switching valve (VICI Valco, Houston, TX) at the column inlets and similar 4-port switching valves in the outlet manifold leading to the detector. In an adsorption experiment on the sorbent column, the desired sample gas mixture can be set using the mass flow controllers and allowed to fully stabilize through the bypass column while the sorbent column is flushed with He via the purge inlet (Figure 2). A single rotation of Valve **D** then interchanges these flows, directing He through the bypass column and presenting the sample mixture to the head of the sorbent column (Figure 1). The resulting

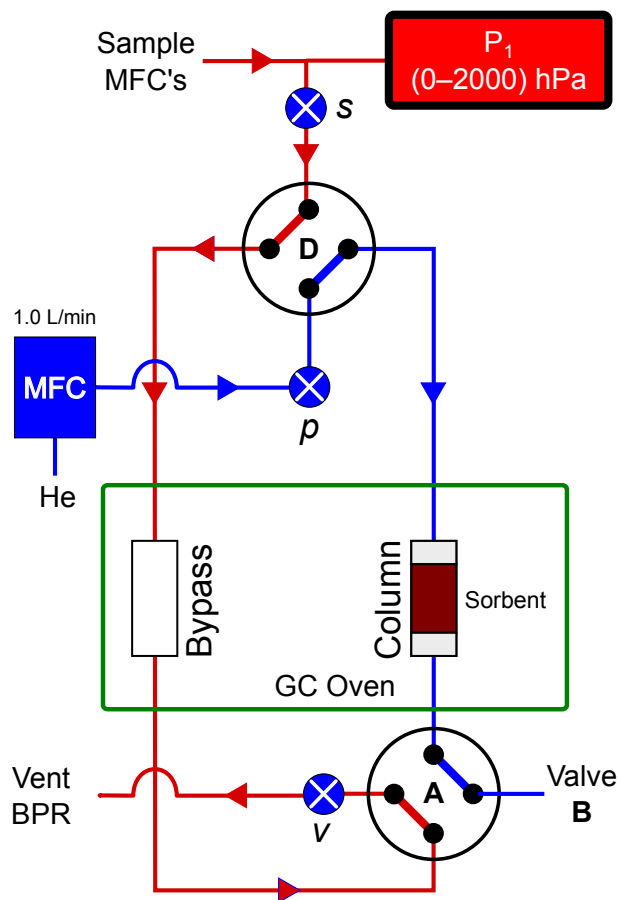


Figure 2: Schematic showing flow patterns of the purge helium (blue) and sample mixture (red) through the columns just prior to rotation of Valve **D** to initiate an adsorption experiment on the sorbent column. Symbols and acronyms are the same as in Figure 1.

concentration profiles at the column heads are extremely sharp, which is important for the DCB analysis.

On the outlet side of the columns, rotary valve **A** controls which of the column exit streams is directed to the detector manifold and which is vented. In experiments, this valve is preset so that the exit stream of the column of interest is directed to the detector. When Valve **D** is switched to initiate an adsorption experiment, the gas composition at the column head undergoes a near step-function change from purge gas to sample gas. This sharp boundary would ideally be maintained all the way to the detector. However, any postcolumn unswept volumes can lead to mixing and longitudinal dispersion of the component concentrations, particularly in shock-like breakthrough curves and blank (bypass) runs. Our use of rotary switching valves in this section eliminates unswept volumes associated with tees in the gas lines. To avoid longitudinal dispersion associated with the postcolumn pressure measurement, Valve **B** can be oriented to isolate the pressure transducer while concentration data are taken, and then rotated to obtain the postcolumn pressure. The postcolumn transducer, P_2 in Figure 1, is the same model used in the input manifold (Mensor CPT6100). The actively-pumped MS inlet, discussed later under the Detector subheading, is designed to minimize the effects of the required tee for sampling.

The employed rotary valves have 4.00 mm ports, which prevent unswept volumes and eddy effects when used with tubing of identical inner diameter (i. d.). The present apparatus utilizes commercially available tubing with a slightly mismatched i. d. of 3.86 mm. This small difference appears insignificant, however, as the shapes of the breakthrough curves were not visibly affected by taper-reaming of the tubing at valve **C** to match the port diameter.

Orientations of the outlet valves (**A**, **B**, and **C** in Figure 1) are set prior to initiation of an experiment and their rotation times are therefore not critical. They are driven by microelectric actuators and rotate in several hundred milliseconds. Inlet valve **D**, however, must rotate rapidly to cleanly initiate an experiment and employs a two-way air actuator driven by a high-speed switching accessory (HSSA, VICI Valco, Houston, TX). This accessory

consists of a pair of solenoid-driven pilot valves that are actuated with He input at 7.1 bar. The high-speed actuator reduces the switching time of Valve **D** to (70 ± 10) ms (measured using the 240 frame-per-second slow-motion video recording of an Apple iPhone 11) and thus minimizes the blockage of flow that occurs during the valve rotation.

A mass flow meter (MFM, Alicat, $1000 \text{ cm}^3 \cdot \text{min}^{-1}$ full scale) is included after the MS sampling to monitor variations in the output flow rate induced by the adsorption. Although we do observe small variations in the flow rate that are similar to the concentration profile, they are small (on the order of 1%, consistent with the adsorptive concentration). At $400 \mu\text{L} \cdot \text{L}^{-1}$ CO_2 concentration, no variation in flow rate is observed, which is consistent with the specifications of the MFM.

Pressures in the system are controlled by a pair of precision backpressure regulators (BPRs) (HF Series, Equilibar, Fletcher, NC). Each BPR is connected to a static reference pressure (the pilot pressure), and the BPR maintains the system pressure at its location at the reference value. The “measurement BPR” (Figure 1) is located immediately after the MFM, and the “vent BPR” is placed in the vent flow after Valve **v**. The inlet pressure of the purge or sample gas at the head of each column is thus controlled by whichever BPR is in the respective flow path, which varies depending on the orientations of rotary valves **A** and **D**. The BPR pilot pressures are controlled individually by absolute-pressure inline regulators (Matheson, Montgomeryville, PA).

The system is pumped at the outlet using a hermetically sealed dry scroll pump (IDP-3, Agilent Technologies, Santa Clara, CA). For simplicity we have elected to actively pump the system at all measurement pressures, although direct venting could have been employed in experiments done above atmospheric pressure. We have performed measurements with and without active pumping and find no differences in the curve shapes or measured capacities.

In experiments, the precolumn sample gas pressure is continuously monitored near the outlet of the input manifold. However, to minimize uncertainties caused by longitudinal dispersion of the postcolumn gases, Valve **B** is oriented during an experiment so that the

postcolumn pressure transducer is isolated from the sample gas flow (as shown in Figure 1) while the concentration data are recorded. After these data are taken and prior to the bypass run, Valve **B** is rotated and the postcolumn pressure is recorded.

Adsorption and desorption runs and their associated blanks are performed by setting valves **D** and **A** such that the rotation of **D** alone will initiate the desired experiment. Because rotation of Valve **D** simultaneously interchanges the flow of purge gas and adsorptive gas mixture between the bypass and sample columns, the order of experiments must be carefully considered. For example, if both adsorption and desorption data on a sorbent are desired, Valve **A** should be set to monitor the sample column outlet concentration and both adsorption and desorption experiments should be performed via rotation of Valve **D**. After these are complete, Valve **A** can be rotated to monitor the bypass column outlet concentrations, and the adsorption and desorption blank runs can be run by rotating Valve **D** as appropriate. Strictly speaking, analogous logic pertains to the bypass runs, but we assume (confirmed by our data) that adsorption on the walls of the empty bypass column is so minimal that no reactivation of this column is required.

Defining experimental time

An adsorption run is initiated by rotation of Valve **D** to direct the sample gas to the column of interest. In the experiment, time zero, t_0 , is defined by the valve rotation event and is matched with the start of concentration data collection by visually noting the corresponding number of the most recent MS scan. However, the true time zero and corresponding species concentration data for a DCB curve relate to sample gas exiting the column and are slightly offset from the experimental observables. There is a slight delay between actuation of Valve **D** and the sample gas passing through the column, and there is an additional small delay between the gas exiting the column and the measurement of concentrations at the MS. Finally, since the MS records scans only every 250 ms and the scan timing is not (presently) linked with rotation of Valve **D**, in every experiment there can be a slight variation in the

matching of the time/concentration data. Fortunately, the above errors are small and are nearly the same in sample and blank runs; they therefore largely cancel in the calculation of adsorption capacity and other parameters of interest. They do, however, need to be considered in the uncertainty analysis, as will be done later.

Pressure Balancing

Ideally the pressure at the head of the column would not change when Valve **D** is rotated. However, differences in flow restriction between the columns can lead to a brief pressure instability at the column head when Valve **D** is rotated. This can be minimized by fine-tuning the pressures at each experimental condition such that the pressure on the vented column matches what the pressure will be on the detected column after valve rotation.⁷

For bypass runs it is straightforward to determine the exact head pressure of the bypass column under the measurement conditions and then make necessary adjustments. Valves **A** and **D** are first oriented so that sample gas is passing through the bypass column and into the detector manifold (i.e. the configuration where the concentration data will ultimately be taken). After noting the pressure at the head of the bypass column (P_1 in Figure 1), Valve **D** is rotated back to the premeasurement configuration, and the vent BPR then adjusted until P_1 in this orientation matches the P_1 value noted earlier to within approximately (0.2 to 0.3) hPa. This ensures that there is little change in the head pressure of the bypass column upon rotation of Valve **D** and minimizes anomalies in the measured blank curve.

When performing an adsorption run on the sorbent column, however, activated sorbent cannot be exposed to the sample gas immediately prior to carrying out the run. For sorbent testing, we therefore determine the head pressure before the sorbent is activated. The procedure is otherwise analogous to that described earlier: after setting the system to the desired pressure and temperature conditions, the sample gas is passed through the (unactivated) sorbent column to the detector manifold and the value of P_1 recorded. Following sorbent activation (during which temperature and flow paths are changed, but not the detector

manifold pressure setting), the system is returned to the previously-selected measurement conditions with the valves oriented in the premeasurement state shown in Figure 2. The vent BPR is then adjusted so that P_1 in this state matches that recorded earlier. The adsorption experiment is now ready to be initiated by rotation of Valve **D**.

The above pressure balancing procedures successfully minimize transient effects on the early-time concentration profiles, as will be more fully demonstrated when breakthrough curves are presented later in this work.

Temperature

Primary temperature control was provided by an Agilent 6890 gas chromatograph (GC) oven. Our previous experience^{8,9} with this and other modern GC's has shown that their oven temperatures are very accurate and stable even at the temperature extremes. This is consistent with the need for accurate and stable absolute temperatures to ensure the reproducibility of gas chromatograph retention times across all instruments. Presently, temperatures were also monitored during the adsorption runs via a Type-K thermocouple probe affixed to the outlet fitting of the sorbent column to ensure that the column had reached a stable temperature after activation was complete and the sample was cooled to the measurement temperature. Nonetheless, in all cases, the thermocouple temperatures stabilized within 1.5 K of the value reported by the GC and had a consistency of better than 0.1 K, the resolution of the thermocouple controller used. These are well within the uncalibrated absolute accuracy of a Type-K thermocouple. Experimental temperatures were taken as the value reported by the GC, which uses a high-accuracy RTD and has a resolution of 1 K.

No attempt was made to monitor the adsorbent bed temperature during an experiment. Any changes are anticipated to be very small given the small sample size, small concentration of CO_2 , and the rapid dissipation of any heat due to the large flow of He, which has an extremely high thermal conductivity.

Detector

Detection of the postcolumn gases is done via a mass spectrometer (MAX-300G, Extrel, Pittsburgh, PA). For sample extraction, a 1.59 mm o. d./0.76 mm i. d. stainless tube is inserted into the 6.35 mm o. d. tubing of a tee located in the loop connecting adjacent ports in Valve **C** (see Figure 1) via a bored-through compression fitting. The inlet of the sampling tube was placed ≈ 5 cm upstream of the sampling tee to eliminate the possibility of unswept volumes affecting the concentration measurements. Depending on the system pressure, approximately $25 \text{ cm}^3 \cdot \text{min}^{-1}$ (IUPAC STP) of gas is removed from the sample stream via a secondary vacuum pump and needle valve, and a fraction of this sample passes into the mass spectrometer via a capillary. After setting the downstream pressure with the measurement BPR, the MS signal is monitored and the needle valve is adjusted so that approximately the same amount of sample is extracted in all experiments, although at the lowest pressures, the needle valve cannot open sufficiently to extract the full amount and sampled volumes are lower (down to $15 \text{ cm}^3 \cdot \text{min}^{-1}$). This affects only signal-to-noise ratio and has no impact on the shape of the measured DCB curve. The remaining sample passes through Valve **C** to the mass flow meter, which measures the remaining flow and is recorded throughout the run. Although not done in a typical experiment, Valve **C** can be rotated to isolate the MS from the remainder of the sampling manifold either to check system mass flows in the absence of sampling or for standby operation.

CO_2 concentrations were determined by monitoring its parent peak at a mass-to-charge ratio (m/z) of 44. N_2 , added to a few mixtures, was monitored at m/z 28. We also routinely monitored for water at m/z 18, although no H_2O signal was observed at any point. Signals were obtained by integrating a ± 1 Da region around the desired m/z , and the MS was restricted to scanning only in the sampled regions. Detector gain was set so that the detector responses for adsorptive equilibrium concentrations were within the linear range. The mass spectrometer was found to maintain excellent concentration stability with no systematic deviation from the constant baseline over at least several hours. Linearity was calibrated

over the range of interest using the mass flow meter manifold to vary concentration.

Chemicals and Sample Activation

Gases used in the system were helium (99.999 % ultrahigh purity, Roberts Oxygen, Rockville, MD), carbon dioxide (99.999 %, ULSI grade, Matheson Gas), and nitrogen (99.999 % ultrahigh purity, Roberts Oxygen, Rockville, MD).

The adsorbent studied was a 13X zeolite provided by Supelco (matrix Molecular Sieve 13X) as a 45 to 60 mesh powder. Samples of approximately 250 mg were placed in a custom column fixture with a plug of quartz wool (typically (10 to 20) mg) at each end of the sample bed to prevent shifting of the zeolite. Cells were capped at each end by 60 μm fritted VCR gaskets (Swagelok) and the bypass and sorbent columns installed with VCR fittings in the flow paths as indicated in Figure 1. Because VCR fittings are zero-clearance, the sample cells can be easily swapped out without otherwise disturbing the setup. Nonetheless, samples were typically not removed from the system until experiments at all desired conditions were completed.

Following installation, each studied zeolite sample was activated *in situ*, initially with a $100 \text{ cm}^3 \cdot \text{min}^{-1}$ flow of He with a $40 \text{ K} \cdot \text{min}^{-1}$ heating ramp to 623.1 K followed by a hold for 16 h. This desorbed any residual water possibly introduced during packing of the column. Thereafter, however, we typically used a less extreme activation for individual runs. Daily, initial activation of the zeolite was for 1 h at 623.1 K and $1000 \text{ cm}^3 \cdot \text{min}^{-1}$ of He at the measurement pressure for the first run, which ranged from approximately (350 to 1100) hPa. For the remainder of each day, the same activation temperature and He flow rate was applied, but the activation time was 900 s. As described below, these activation procedures were tested and found to be adequate for the currently studied conditions. The longer daily first-run activation was precautionary, but we saw no evidence that the longer time was necessary. When not in use, columns were pressurized with purge He above atmospheric pressure and sealed off by closure of appropriate diaphragm valves of the apparatus. Prior

to the experimental runs, samples were held at the measurement temperature for at least 600 s and temperatures were confirmed with a K-type thermocouple mounted outside the sample cell.

A 900 s activation time is atypically short for a 13X zeolite; however, we have found for these dry samples that a longer activation was not necessary and did not significantly affect the measured capacities. Compared with results with a 900 s activation time, a 300 s activation time gave capacities only a few percent lower. Measurements were also taken after an overnight activation [(14 to 16) h at 623.1 K and a $100 \text{ cm}^3 \cdot \text{min}^{-1}$ flow of He]; no significant difference in capacity was observed compared with a 900 s activation. Samples were not exposed to anything except (dry) sample gas or UHP He after they were placed into the sample cell and initially activated. The abbreviated activation schedule used in this work is likely insufficient for a sample exposed to H_2O , which binds much more strongly to zeolites than the compounds used in this work.

Results and Discussion

To characterize the system and to evaluate its reproducibility, we have measured breakthrough curves and derived CO_2 adsorption capacities for a 13X zeolite over a range of temperatures and pressures that are representative of the troposphere. These initial validation studies employ conditions that are conducive to rapid analysis and use simplified mixtures to allow a clear assessment of the instrument without complicating assumptions.

The majority of the breakthrough measurements were carried out with a $(1.00 \pm 0.01) \%$ mixture of CO_2 in helium, utilizing total flow rates of $(500 \pm 3) \text{ cm}^3 \cdot \text{min}^{-1}$ (IUPAC STP), where uncertainties are derived from the mass flow meters at four temperatures, 233.1 K, 273.1 K, 298.1 K and 323.1 K and three nominal pressures 350 hPa, 700 hPa and 1100 hPa. We elected to use He and not air as the bath gas to minimize the possibility of interference from N_2 and O_2 , although extensive previous work^{10–13} has shown little general impact of

N₂ and O₂ on CO₂ adsorption capacity in 13X zeolite at low pressures.

In addition to the studies with a 1 % mixture of CO₂ in helium, a few experiments employed a much lower CO₂ concentration of 400 μL·L⁻¹ and, in other tests, a 1 % mixture of N₂ in helium was studied to examine transient pressure artifacts. The present measurements utilized a sorbent column sized to contain approximately 250 mg of sorbent. This results in experiments of convenient duration, and the small amount demonstrates the suitability of the instrument for testing new candidate sorbents that may be available in limited quantities.

Breakthrough Curves

Figure 3 shows three breakthrough curves at (a) low capacity (i. e. high temperature and low pressure), (b) moderate capacity, and (c) the highest capacity (low temperature and high pressure). Prior to each experiment, the 623.1 K activation procedure described previously was utilized to completely remove the adsorbed CO₂. Pressures shown in the figure are mean pressures between the column head and outlet; pressure drops were significant (up to 171.4 hPa at the highest temperature and lowest pressure) and depend on temperature and measurement pressure as discussed below.

The breakthrough curves themselves are consistent with a Type I adsorption isotherm, as expected for a 13X zeolite.¹⁴ The small angular feature at 210 s in the lowest temperature experiment (curve c) is reproducible. We attribute the slight abruptness to minor adsorption of the initial breakthrough CO₂ on the 233.1 K walls downstream of the column. The difference in capacity will be compensated in the blank run, which is subject to the same temperature, but a slight compensation would be required for an analysis of the breakthrough curve shape at these early times.

The concentration profiles observed in the blank runs should be very similar to those presented to the sorbent column at the same temperature and pressure. The curve shapes, which would ideally be step functions, reflect any flow anomalies and any longitudinal diffusion, from the head of the column to the detector. In the absence of pressure balancing

procedures (see Experimental section), brief spikes of several second duration in the blank column CO₂ concentration profiles are observed. These arise if the column head pressure shifts when Valve **D** is rotated. They are essentially absent in the pressure-balanced runs of Figure 3, wherein the blank column curves are extremely sharp, rising from 10 % to 90 % of full value over (2.0 to 4.5) s.

In the present work the fastest rise time, defined as the time required for the concentration to increase from (10 to 90) % of the equilibrium concentration, occurs at low pressures with virtually no temperature dependence, whereas the highest pressures show the next fastest rise times, also with little variation with temperature (complete data for all runs is provided in Table S1 in supporting information). The middle pressures display the slowest rise times and a slight positive dependence on temperature. The measured rise times are somewhat anomalous with the expected effects of temperature and pressure, in that one would anticipate the rise time to monotonically increase with pressure due to the velocity decrease that occurs with increasing pressure under the applied constant mass flow conditions. The observed behavior is more complex. Diffusion effects will be superimposed on the direct impact of velocity and should also be considered. Since $\langle d \rangle = \sqrt{2Dt}$, where D is the diffusion coefficient, t is time, and $\langle d \rangle$ is the root-mean-square distance a molecule will travel in time t , the dispersion effects of diffusion partially cancel. In particular, the inverse linear dependence of D on pressure under the present conditions¹⁵ completely compensates for the increased time in the tube due to the lower velocity. Only the temperature dependence¹⁶ of $D \propto T^{1.72}$ will change, leading to $\langle d \rangle \propto T^{0.86}$. The data of Table S1 are ambiguous, however, regarding the impact of temperature. The lack of total consistency in the rise-time trends may reflect measurement scatter combined with slight variations in the pressure balancing precision, temperatures, or wall adhesion. In any case, since they represent extremely small variations in capacity and will have no significant effect on the shape of the corrected breakthrough curves, the rise times are not considered further.

Irrespective of such details, the extremely sharp blank column curves show that dispersion

and other flow anomalies are largely avoided, and that column outlet concentrations are well-mapped to the MS detector. The observed CO₂ profiles are very close to the ideal square wave desired for DCB experiments.

CO₂ flow in sorbent column runs is subject to pressure artifacts and dispersion effects similar to those described for the bypass column. These are not readily observable in sorbent column runs, however, because complete CO₂ adsorption is initially occurring. Flow behavior in sorbent column runs was further evaluated by using a 1% mixture of N₂ in helium to probe the N₂ profiles. Since N₂ is minimally adsorbed under our conditions (Table 1) by 13X zeolite,^{11–13,17,18} effects on its concentration profile due to any flow anomalies should be evident and correspond similarly to variations in the concentration profile of CO₂ in the very early times of the adsorption experiment. Shown in Figure 4 is the sorbent column N₂ profile and its corresponding N₂ blank run. With good pressure balancing, the sorbent column experiment correlates nearly identically with the blank run. To probe the effect of pressure balancing, a set of experiments with slightly offset column head pressures was carried out (Figure S1 in supplemental information). We find that deviations of more than ≈ 0.5 hPa cause small visible artifacts in the early N₂ profiles and that effects systematically vary with the direction and magnitude of the pressure difference. In corresponding mixtures, CO₂ profiles at the column head are expected to exhibit similar variation. Given that such disruptions are small in pressure-balanced experiments and occur over only a tiny fraction of the total adsorption time, they will minimally affect derived CO₂ adsorption capacities.

Finally, to demonstrate capabilities of the present apparatus at low CO₂ concentrations, Figure 5 shows bypass and sorbent column DCB curves obtained at 298.1 K and 1043.1 hPa with a sample mixture containing only 400 $\mu\text{L}\cdot\text{L}^{-1}$ CO₂. The curves are very similar in quality to those obtained with CO₂ concentrations of 10 000 $\mu\text{L}\cdot\text{L}^{-1}$. Although these measurements were run at a higher gain setting on the MS amplifier than those that utilized 1% CO₂ mixtures, the observed signal-to-noise ratio is still excellent.

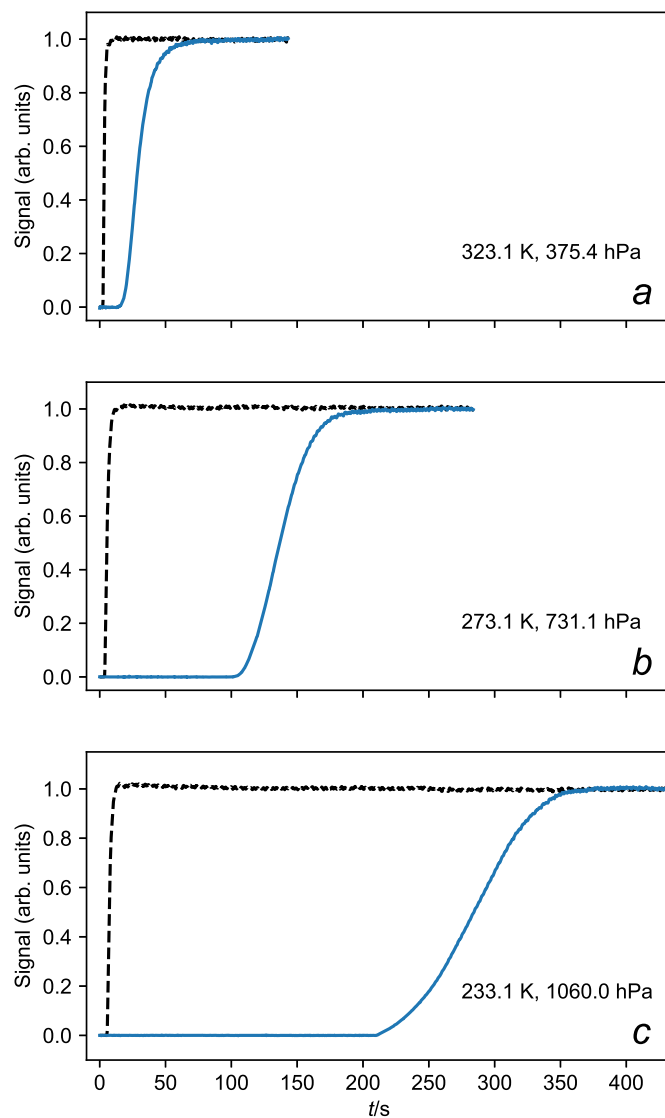


Figure 3: Dynamic column breakthrough curves for CO₂ on 249 mg of 13X zeolite exposed to 1.000% CO₂ in He at 500 cm³ · min⁻¹ (IUPAC STP) at the indicated temperatures and mean total pressures; shown are the MS (m/z) 44 signals obtained for the sorbent column (blue solid curves) and the blank (black dashed curves); temperatures and average pressures are as indicated.

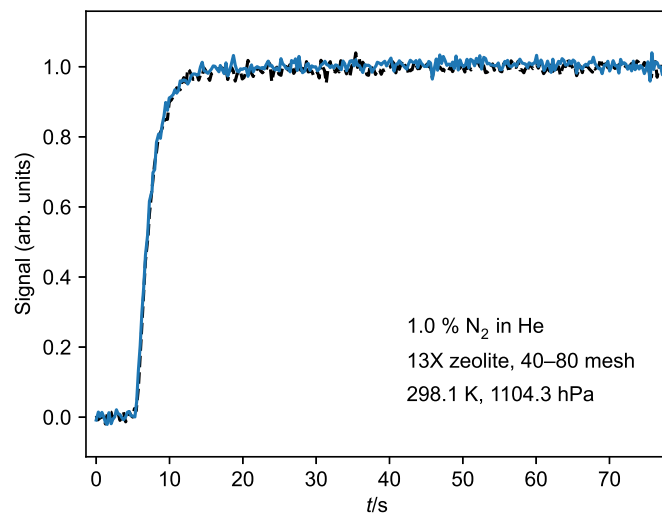


Figure 4: Dynamic column breakthrough curves for N_2 on 249 mg of 13X zeolite exposed to 1.00 % N_2 in He at $500 \text{ cm}^3 \cdot \text{min}^{-1}$ (IUPAC STP) at 298.1 K and mean total pressure 1104.3 hPa; shown are the MS (m/z) 28 signals (see text) obtained for the sorbent (blue solid curve) and blank (black dashed curve) runs.

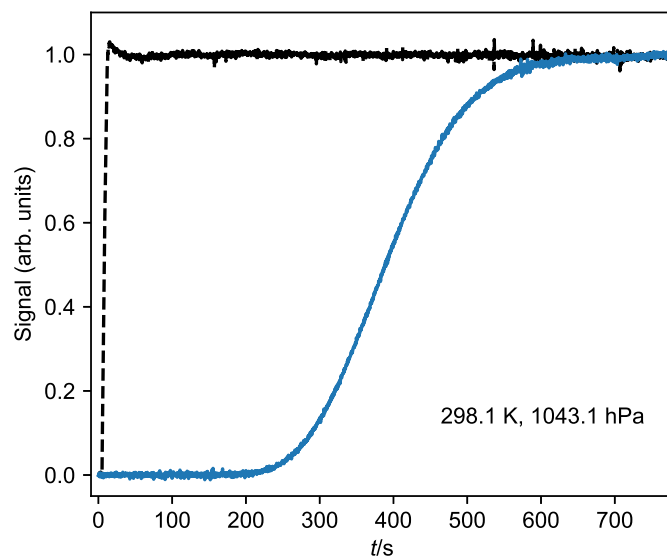


Figure 5: Dynamic column breakthrough curves for CO_2 on a 13X zeolite exposed to $400 \mu\text{L} \cdot \text{L}^{-1}$ CO_2 in He at $500 \text{ cm}^3 \cdot \text{min}^{-1}$ (IUPAC STP); shown are the MS (m/z) 44 signals obtained for the sorbent column (blue solid curve) and the bypass (black dashed curve); temperature and mean total pressure are as indicated. The measured capacity under these conditions is $0.23 \text{ mol} \cdot \text{kg}^{-1}$; static adsorption isotherm measurements (see text) yield $0.22 \text{ mol} \cdot \text{kg}^{-1}$.

Adsorption Capacity

Because sorbent capacity can be measured directly without using models for adsorption, transport, kinetics, etc., our initial analysis has focused on determining the capacity of an adsorbent under specific experimental conditions. In the present experiments, the use of a downstream backpressure regulator allows the outlet concentration measurements of the bypass and sample columns to be made at the same fixed absolute pressure, irrespective of gas composition or flow velocity. In this case, the measured saturated adsorbate signal s_{in} from the bypass column exactly reflects the inlet mole fraction at the head of both the bypass and sample columns. Therefore, for single adsorbate systems, the ratio of the time-dependent adsorbate signal, $s(t)$, to s_{in} represents the fraction of the inlet adsorbate that passes through the column and will be unity once saturation occurs. As discussed by Wilkins, et al.,⁷ this lies in contrast to the ratio of concentrations at the inlet and outlet, which varies depending on the pressure variation across the length of the column.

The CO₂ breakthrough curves of the sample and bypass start at the purge gas CO₂ concentration (very low in ultra-high purity He) and end at s_{in} , its concentration in the inlet gas. As a result, the single-component equilibrium adsorption capacity, q_e can be determined via

$$q_e = \frac{Q_{\text{in}}(t_f - t_0)}{ms_{\text{in}}} \left[\int_{t_0}^{t_f} s^{\text{b}}(t) dt - \int_{t_0}^{t_f} s^{\text{s}}(t) dt \right], \quad (1)$$

where $s^i(t)$ are breakthrough curves for the sample ($i = \text{s}$) and bypass ($i = \text{b}$) columns, t_0 is the valve rotation time, defined above, t_f is an arbitrary time at which the concentrations of both curves have reached the inlet concentration s_{in} , m is the mass of sorbent, and Q_{in} is the input adsorptive molar flow rate. In the present work, Q_{in} is calculated from the mass flow meter settings of pure gases assumed to be ideal. These data are reported in Table 2.

Once the sample gas has fully saturated the sorbent column, a desorption curve can be measured by rotating Valve **D** to switch the gas flowing through the column from sample gas back to the purge gas while monitoring the time-dependence of the concentrations in

Table 2: Measured adsorbent capacities of CO₂ on 13X zeolite over a range of temperatures (T) and total pressures (P). Pressure represents the mean of the inlet and outlet pressures with ΔP representing the pressure difference between the inlet and outlet of the sorbent column. q_e^{DCB} and q_e^{static} are the molar capacities measured by the present apparatus and an independent static adsorption isotherm measurement, respectively, as discussed in the text. The partial pressure of CO₂ is 1% of the total pressure. The relative standard uncertainty for the measurements (u_r) is 0.05.

| T (K) | P (hPa) | (ΔP) (hPa) | q_e^{DCB} (mol · kg ⁻¹) | q_e^{static} (mol · kg ⁻¹) |
|---------|-----------|--------------------|--|---|
| 233.1 | 350.5 | 105.7 | 3.47 | |
| 233.1 | 721.2 | 53.1 | 3.93 | |
| 233.1 | 1060.0 | 34.3 | 4.18 | |
| 273.1 | 359.42 | 131.64 | 1.58 | 1.55 |
| 273.1 | 731.1 | 68.9 | 2.04 | 1.95 |
| 273.1 | 1068.3 | 48.4 | 2.19 | 2.17 |
| 298.1 | 358.7 | 143.7 | 0.88 | 0.87 |
| 298.1 | 729.4 | 70.9 | 1.22 | 1.19 |
| 298.1 | 1077.9 | 56.2 | 1.36 | 1.37 |
| 323.1 | 375.4 | 171.4 | 0.41 | 0.42 |
| 323.1 | 743.6 | 89.1 | 0.62 | 0.65 |
| 323.1 | 1068.5 | 57.9 | 0.75 | 0.78 |

the exit stream. Similar to the adsorption case, the desorption curves of the sample and its associated blank curve can be integrated to derive the amount of desorbed material and can be compared with the quantity obtained from the adsorption measurements. Initial studies nominally suggest the release of only $\approx 80\%$ of the adsorbed CO₂ even under gentle heating to 313.1 K; however, the capacity derived from desorption is extremely sensitive to the initial timing since the signal monotonically decreases after switching to purge gas. Small changes in the initial integration point result in a complete recovery of the amount of sample adsorbed, and we attribute the observed difference to reflect our time uncertainty (see below) combined with the high sensitivity to this uncertainty in the desorption runs. As a result, we have elected to determine capacities only using adsorption runs.

To evaluate the absolute measurement of capacity, we have compared the present results at 273 K, 298 K and 323 K to static measurements (Figure S3 in supplemental information) taken at NIST with a manometric adsorption analyzer (Autosorb iQ MP, Quantachrome Instruments, Boynton Beach, FL). At all temperatures and pressures, the present values

reproduced capacities derived by interpolation of the static measurements to within $\pm 4.5\%$, which is within the uncertainty limits of the present experiments with breakthrough times of only a few minutes. Note that the above comparison makes no provision for the uncertainty in the static measurements themselves, particularly for temperatures that deviate from 298.1 K. As discussed below, the uncertainties in capacity from the DCB apparatus primarily derive from uncertainty in timing of the valve rotation relative to the corresponding the MS scan (i.e. t_0). The absolute uncertainty in time is constant, so that shorter breakthrough times have larger relative uncertainties. The capacities reported in Table 2 were obtained with CO_2 concentrations of $10\,000\ \mu\text{L} \cdot \text{L}^{-1}$; longer breakthrough times, such as with $400\ \mu\text{L} \cdot \text{L}^{-1}$ CO_2 breakthrough curves, are expected to have lower uncertainty, although the lower capacity expected at lower partial pressure offsets most or all of the difference. The CO_2 capacity derived from the $400\ \mu\text{L} \cdot \text{L}^{-1}$ CO_2 DCB curve of Figure 5 is $0.23\ \text{mol} \cdot \text{kg}^{-1}$, compared with a value of $0.22\ \text{mol} \cdot \text{kg}^{-1}$ derived from static adsorption measurements. The 4.3% difference is very similar to that typically observed in Table 2.

Useful comparison of the present results with literature data on 13x zeolite is limited by the expected variation of the CO_2 capacity with the zeolite origin. Nonetheless, our measurements are broadly consistent with values derived from the Toth-model isotherms reported by Wang and LeVan¹⁹ from pure component equilibrium studies of CO_2 on an alternatively sourced 13X zeolite (Grace Davison, MS-544HP) using volumetric and gravimetric methods.

Uncertainty Analysis

The uncertainty in the measured adsorption capacity is expected to be dominated by the uncertainty in timing of the sample gas front arrival. As described above, scans are recorded with ≈ 250 ms spacing, and Valve **D** is estimated to rotate in (60 to 80) ms. Currently, no electronic provision for timing the specific MS scan number to the valve rotation is available. As a result, timing is set by visually noting the scan number when Valve **D** is actuated to initiate the experiment. We estimate the primary errors are in the relative and absolute

correspondence of gas front timing to valve actuation and MS data collection, with variations caused mainly by the operator and the processing of the serial control commands for the valve actuator.

As an initial estimate for the Type A uncertainty^{20,21} of the individual runs, we have analyzed the onset times for adsorption blank runs spanning several runs. The breakthrough curves for these bypass runs are extremely sharp as expected, and the variation in these runs should be a good estimate of the individual run-to-run variation. These were found to span 0.8 s at half-maximum height, leading to a conservative estimate of a possible random deviation of 4 scans from the recorded scan (the valve is actuated after the recorded scan is shown on the MS). In the analysis, adjusting the timing of the adsorption run or the bypass run by 4 scans yielded a relative uncertainty estimate of $u_r = 0.04$ for the derived capacity. Note that this assessment is obtained by arbitrarily placing the maximum deviation only the bypass curve, despite the likelihood of some correlation (due to constant delays in the system and a single operator), and is likely an upper estimate.

Additional Type A uncertainty comes from the noise in the MS signal. The time at which breakthrough is deemed to be complete, t_f , is arbitrary once the average value of the signal reaches a constant value. We can estimate the noise uncertainty by calculating the capacity using widely varying values of t_f . In doing so, we estimate the relative uncertainty due to the noise to be approximately $u_r = 0.03$, leading to an estimated total Type A uncertainty in the capacity measurement of $u_r = 0.05$. Note that this value is for the present measurements using 1 % CO₂ mixtures, conditions that yield breakthrough times (i.e. the lowest acceptable value of t_f) of (2 to 5) min.

Type B uncertainty in the time may be evaluated by the absolute time difference between the valve actuation and arrival of the gas front at the detector. When Valve **B** is open to the pressure transducer, an additional 71 cm of tubing is introduced into the stream, which is found to shift the curve 1.6 s later at 500.0 cm³ · min⁻¹ (IUPAC standard volumetric flow) and 1.20 bar pressure. The interior diameter of these tubes over most of their length is

3.86 mm, leading to an estimated velocity of $65.8 \text{ cm} \cdot \text{s}^{-1}$ at a room temperature of 296 K. The additional length would be expected to add 1.1 s. The additional 0.5 s observed is due to relatively constant delays for serial control commands, solenoid charging and actuation, pilot valve actuation, and valve rotation. More detailed modeling might slightly improve this number; however, we expect this variation to remain constant between adsorption and bypass runs, thus minimizing the impact. Based on this constant variation between runs and the small absolute value, we estimate the Type A uncertainty to dominate the Type B uncertainty and thus report all capacity uncertainties as relative standard uncertainties, $u_r = 0.05$.

Another potential area of uncertainty is derived from the large pressure drop across the column at the flow rates used in this experiment. Our current analysis assumes that the measured CO_2 adsorption capacity pertains to a simple average of the inlet and outlet pressures in each experiment. As a point of comparison, the CO_2 adsorption isotherm for the presently studied 13X zeolite was independently measured in the NIST Facility for Adsorbent Characterization and Testing (FACT) lab at 298 K using a manometric adsorption analyzer and shows curvature over the CO_2 partial pressures of the present experiments. We have fit the FACT lab data (Figure S4 in supporting information) to a Sips-modified Langmuir (SML) isotherm,²² and used the result to estimate the variation of adsorption capacity over the pressure drops observed in the breakthrough experiments at 298 K. Compared with simple pressure averaging, we find that using the SML isotherm leads to capacities that are 0.91 % smaller in the experiments near 350 hPa, which is where the largest pressure drops occur in this work (Table 2). This difference, however, is much less than the uncertainty estimated above from other error sources, and is therefore not considered further.

Other sources of uncertainty are absolute flow rates ($u_r < 0.01$) and the CO_2 concentration ($u_r = 0.01$) in that flow and are dominated by the time and noise uncertainties. Pressure measurements are accurate to within 0.2 hPa below 1000 hPa and 0.01 % above, according to the manufacturer. The sorbent mass was measured using a balance with a resolution of

0.0001 g, although we report to the nearest 0.001 g to account for possible uptake of ambient H₂O during sample preparation.

Extra Column Volume

Extra column volume (ECV) refers to all volumes in the system outside of that contained in the column itself and has been a source of significant concern.^{5,13,23,24} It is often referred to as “dead” volume, presumably as a parallel to language used in describing static adsorption studies, although in other fields “dead volume” often only refers to unswept volumes in a flow stream.

In any case, as noted by Wilkins et al.,⁵ the ECV’s differ in treatment precolumn and postcolumn. In the precolumn region, longitudinal dispersion at the interface of the purge and sample gases affects the presentation of a step function to the head of the column. In the present work, the use of a single rotary valve (Valve **D** in Figure 1) to switch the parallel input streams and initiate the experiments, mitigates many of these effects. After Valve **D**, unswept volumes will also affect the square wave profile, and the sample cell in the present apparatus incorporates a tee for future flexibility in studying the sorbent bed (e. g. temperature measurement). The CO₂ signal profiles through the bypass column (Figure 3) are indicative of the concentration pulse at the head of the column and are very close to the desired square wave.

The postcolumn ECV poses additional challenges due to changing concentrations and flow velocity during the breakthrough measurements. Wilkins et al.⁷ approach this by removing all postcolumn connections between the sorbent column and detector, which is effective but would, among other limitations, prevent the measurement of the downstream pressure prior to the MS in the present apparatus, which is necessary because the MS removes sample from the flow stream. In large part, the use of the 4-port, 2-position chromatography valves minimizes the impact of these changes because no unswept volumes are present to induce concentration changes beyond those from the column itself. In addition, eddies that might

induce intracolumn mixing are also minimized by matching the port sizes to the tubing inner diameter. In the present system, we observe a very close mapping of the concentration at the column outlet to the detector, despite a relatively large volume downstream of the column.

The use of rotary valves in a DCB apparatus is not unique,^{7,25,26} and Wilkins et al.⁷ specifically utilize a similar input rotary valve to initiate the breakthrough experiment. In that apparatus, the pressures readings on the inlet mass flow controllers are used to adjust BPRs to match pressures in their equivalent sample and bypass legs. However, we have found that the mass flow controllers must be configured so that the control valve is on the outlet side to achieve acceptable concentration stability under the low concentrations used in the present system. The measured pressure on the flow meters is therefore the regulated gas pressure, and we have thus used separate pressures gauges (P_1 and P_2 in Figure 1). Use of the mass flow controllers in a configuration with the control valves on the inlet side required many hours of flow to achieve a stable concentration as measured by the MS.

Conclusion

The apparatus described in this work is focused on meeting requirements for the characterization of DAC sorbents specifically. We have demonstrated the ability of the system to accurately measure adsorption capacities over a wide range of atmospherically relevant temperatures and pressures under dry conditions at concentrations as low as $400 \mu\text{L} \cdot \text{L}^{-1}$ and samples on the order of a few hundred milligrams.

The methodology compares the DCB curves of two columns that are identical other than one containing a sorbent. Using a fast-opening rotary valve to switch purge and sample gases between the columns leads to inlet concentration profiles very close to the ideal square wave desired in DCB experiments. We find it is necessary to closely match the pre- and post-rotation column head pressures to avoid brief pressure artifacts in the early concentration profiles. By utilizing rotary valves and matching tubing diameters in the entire postcol-

umn manifold, we minimize dispersion and show excellent mapping of the column outlet concentration to the detector while maintaining the ability to measure postcolumn pressure.

From a detailed analysis, overall uncertainties in the present measurements are found to be dominated by the relative and absolute timing of the arrival of the sample gas fronts to the columns and detector. We look forward to improving the accuracy of the instrument while maintaining a rigorous uncertainty evaluation. Future work will focus on extending the capability of the apparatus to include humidity in order to fully cover the conditions necessary for effective characterization of DAC sorbents as presented in Table 1. This will necessitate a more comprehensive analysis to account for dynamic flow variations caused by component adsorption and concomitant gas viscosity changes.

Acknowledgement

The authors warmly thank Craig Brown for helpful discussions throughout the development of the apparatus. This work was performed as part of the NIST Carbon Dioxide Removal Program (Program Coordinator Pamela M. Chu)

Supporting Information Available

Blank rise times, complete breakthrough curves, adsorption isotherms, and variations in the blank lineshapes due to intercolumn pressure differentials is available as supporting information.

References

- (1) Sanz-Pérez, E. S.; Murdock, C. R.; Didas, S. A.; Jones, C. W. Direct capture of CO₂ from ambient air. *Chem. Rev.* **2016**, *116*, 11840–11876.

- (2) Lackner, K. S.; Azarabadi, H. Buying down the cost of direct air capture. *Ind. Eng. Chem. Res.* **2021**, *60*, 8196–8208.
- (3) Bergman, A.; Rinberg, A. In *CDR Primer*; Wilcox, J., Kolosz, B., Freeman, J., Eds.; 2021; Chapter The case for carbon dioxide removal: From science to justice.
- (4) Seidel-Morgenstern, A. Experimental Determination of Single Solute and Competitive Adsorption Isotherms. *J. Chromatogr. A* **2004**, *1037*, 255–272.
- (5) Wilkins, N. S.; Rajendran, A.; Farooq, S. Dynamic column breakthrough experiments for measurement of adsorption equilibrium and kinetics. *Adsorption* **2021**, *27*, 397–422.
- (6) Certain commercial materials and equipment are identified in this paper in order to specify adequately the experimental procedure. In no case does such identification imply recommendation of or endorsement by the National Institute of Standards and Technology, nor does it imply that the material or equipment is necessarily the best available for the purpose.
- (7) Wilkins, N. S.; Sawada, J. A.; Rajendran, A. Quantitative microscale dynamic column breakthrough apparatus for measurement of unary and binary adsorption equilibria on milligram quantities of adsorbents. *Ind. Eng. Chem. Res.* **2022**, *61*, 7032–7051.
- (8) McGivern, W. S.; Manion, J. A. Extending reversed-flow chromatographic methods for the measurement of diffusion coefficients to higher temperatures. *J. Chromatogr. A* **2011**, *1218*, 8432–8442.
- (9) McGivern, W. S.; Manion, J. A. Hydrocarbon binary diffusion coefficient measurements for use in combustion modeling. *Combust. Flame* **2012**, *159*, 3021–3026.
- (10) Cavenati, S.; Grande, C. A.; Rodrigues, A. E. Adsorption equilibrium of methane, carbon dioxide, and nitrogen on Zeolite 13X at high pressures. *J. Chem. Eng. Data* **2004**, *49*, 1095–1101.

- (11) Park, Y.-J.; Lee, S.-J.; Moon, J.-H.; Choi, D.-K.; Lee, C.-H. Adsorption equilibria of O₂, N₂, and Ar on carbon molecular sieve and zeolites 10X, 13X, and LiX. *J. Chem. Eng. Data* **2006**, *51*, 1001–1008.
- (12) Hefti, M.; Marx, D.; Joss, L.; Mazzotti, M. Adsorption equilibrium of binary mixtures of carbon dioxide and nitrogen on Zeolites ZSM-5 and 13X. *Microporous Mesoporous Mater.* **2015**, *215*, 215–228.
- (13) Wilkins, N. S.; Rajendran, A. Measurement of competitive CO₂ and N₂ adsorption on Zeolite 13X for post-combustion CO₂ capture. *Adsorption* **2019**, *25*, 115–133.
- (14) Mazzotti, M.; Rajendran, A. Equilibrium theory-based analysis of nonlinear waves in separation processes. *Annu. Rev. Chem. Biomol. Eng.* **2013**, *4*, 119–141.
- (15) Reid, R. C.; Prausnitz, J. M.; Poling, B. E. *The Properties of Gases and Liquids*, 4th ed.; McGraw-Hill: New York, 1987.
- (16) Marrero, T. R.; Mason, E. A. Gaseous diffusion coefficients. *J. Phys. Chem. Ref. Data* **1972**, *1*, 3–118.
- (17) Deng, H.; Yi, H.; Tang, X.; Yu, Q.; Ning, P.; Yang, L. Adsorption equilibrium for sulfur dioxide, nitric oxide, carbon dioxide, nitrogen on 13X and 5A zeolites. *Chem. Eng. J.* **2012**, *188*, 77–85.
- (18) Avijegon, G.; Xiao, G.; Li, G.; May, E. F. Binary and ternary adsorption equilibria for CO₂/CH₄/N₂ mixtures on Zeolite 13X beads from 273 to 333 K and pressures to 900 kPa. *Adsorption* **2018**, *24*, 381–392.
- (19) Wang, Y.; LeVan, M. D. Adsorption equilibrium of carbon dioxide and water vapor on Zeolites 5A and 13X and silica gel: pure components. *J. Chem. Eng. Data* **2009**, *54*, 2839–2844.

- (20) Taylor, B. N. *guidelines for evaluating and expressing the uncertainty of NIST measurement results*; 1994; p NBS TN 1297.
- (21) Possolo, A. *Simple guide for evaluating and expressing the uncertainty of NIST measurement results*; 2015; p NIST TN 1900.
- (22) Sips, R. On the structure of a catalyst surface. *J. Chem. Phys.* **1948**, *16*, 490–495.
- (23) Rajendran, A.; Kariwala, V.; Farooq, S. Correction procedures for extra-column effects in dynamic column breakthrough experiments. *Chem. Eng. Sci.* **2008**, *63*, 2696–2706.
- (24) Joss, L.; Mazzotti, M. Modeling the extra-column volume in a small column setup for bulk gas adsorption. *Adsorption* **2012**, *18*, 381–393.
- (25) Hofman, P. S.; Rufford, T. E.; Chan, K. I.; May, E. F. A dynamic column breakthrough apparatus for adsorption capacity measurements with quantitative uncertainties. *Adsorption* **2012**, *18*, 251–263.
- (26) Saleman, T. L. H.; Watson, G. C. Y.; Rufford, T. E.; Hofman, P. S.; Chan, K. I.; May, E. F. Capacity and kinetic measurements of methane and nitrogen adsorption on H⁺-mordenite at 243 – 343 K and pressures to 900 kPa using a dynamic column breakthrough apparatus. *Adsorption* **2013**, *19*, 1165–1180.

TOC Graphic

